

Model for Simulating Yarn Unwinding from Packages

Abstract

Yarn unwinding from packages plays an essential role in many textile processes. The stability of unwinding has a direct influence on the efficiency of the textile processes in general and on the quality of the final products. Calculations based on a theoretical model of unwinding can help us in our pursuit of an optimal design of packages and an optimal unwinding process. We will derive expressions for the time dependence of the angular velocity of the balloon rotation around the package axis, of the unwinding velocity and the winding angle during yarn unwinding from the cylindrical package. We will demonstrate a mathematical model for simulating the unwinding from cylindrical packages. We will show how the winding angle influences the angular velocity and tension oscillations of the yarn during unwinding. Since the centrifugal forces on the yarn in the balloon depend on the angular velocity, this velocity has a large influence on the tension that we wish to reduce.

Key words: winding angle, apex angle, yarn unwinding, yarn angular velocity, package design, new-generation packages.

Introduction

Oscillations in the yarn tension during yarn unwinding from stationary packages have a direct influence on the quality of the fabric. Characteristics of the unwinding process are thus important for the production of high quality garments and should therefore be optimised. The theory of yarn dynamics during unwinding was developed as early as the 1950's [1, 2]. It was upgraded in the 1970's [3, 4] and is still an active area of research [5 - 13]. The theory was recently compared with experimental results with considerable success [14], which demonstrates that theoretical modelling of the yarn unwinding process can be used to simulate and then optimise the parameters of package construction and the unwinding process. In our previous work [15] we showed how such a mathematical model can be devised and we described some general characteristics of the unwinding process. In this work we review the results of our extensive simulations and show how the unwinding properties of a package can be improved by using alternating layers wound in parallel and cross wound.

Model of unwinding simulation

In order to be able to compare various package designs, it is necessary to determine the influence of the winding angle and the apex angle of the package on the angular velocity of yarn forming the balloon, since the angular velocity determines the yarn tension to a great extent. In packages of a general shape (cylindrical or conical) the relation between the angular velocity ω of the yarn during unwinding, the unwinding speed V and

the package radius c at the lift-off point, where the yarn lifts off from the package surface, is [2]:

$$\omega = \frac{V \cos \phi}{c (1 - \cos \alpha \sin \phi)} \quad (1)$$

Here ϕ is the winding angle and is the apex angle of the conical package for cylindrical packages, we put $\alpha = 0$ [2] as follows:

$$\omega = \frac{V \cos \phi}{c (1 - \sin \phi)} \quad (2)$$

In deriving this expression we neglected the variation in yarn length in the balloon during the time interval when the two layers unwind. The dimensionless angular velocity can obviously be expressed as [5]:

$$\Omega = \frac{\cos \phi}{1 - \sin \phi} \quad (3)$$

Typical cylindrical or conical packages consist of layers of yarn with an alternating winding angle ϕ : in one layer it is positive and in the next layer it is negative (**Figure 1**) [14]. The steady-state angular velocity ω depends on the winding angle, and in a simple approximation it is given by **Equation 1**. We can presume that the winding angle is approximately constant in the middle of

the package, but it changes at the edges of the package, where its sign is reversed.

To describe the time dependence of the winding angle, we must look for a periodic function, because the motion of the point must be periodic for good approximation. The most known periodic functions are trigonometric, such as the sine function, which should be modified so that it will change only slightly when the point moves up or down the packages. We can achieve this by raising the sine to a low fractional power, say $1/40$ (we have to be careful about the signs, thus we take an absolute value of the sine function and restore the sign using the signum function:

$$f(t) = \text{sign}(\sin t) |\sin t|^{1/40} \quad (4)$$

Function $f(t)$ has the properties required, and thus it is a good model for the description of cylindrical packages. Speaking of the unwinding process, we are mostly interested in the maximal tensions in the yarn and oscillations of the tension as a function of the unwinding speed. We aim to achieve the highest possible speed, while keeping the tension in the yarn and oscillations as low as possible.

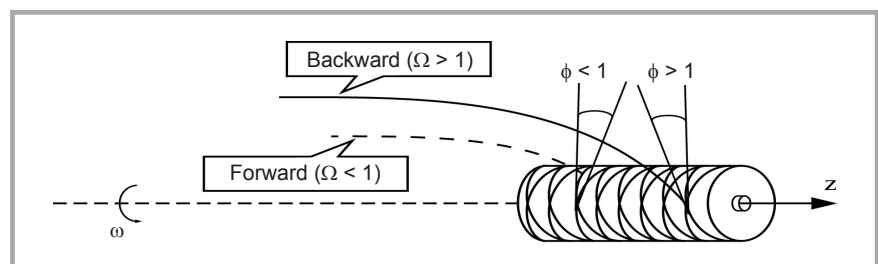


Figure 1. Winding angle during unwinding in the backward and forward directions.

However, we also need a relation between the angular velocity and tension in the yarn. The tension is largest in the eyelet through which the yarn is being pulled [5], being a convenient point to perform experimental measurements of the tension. In the following, when we use the word ‘tension’, we refer to that at the eyelet, denoted by T .

Yarn is unwound from a horizontal package on which it is wound in parallel (**Figure 2**). To limit the tension in the yarn, we used a balloon limiter made out of eight teflon rings. When the yarn leaves the packages it runs through the first guide and tension sensor. Then it goes through the second guide and the unwinding device. Finally it is wound on another package. For packages wound in parallel we have $\alpha = 0$ and $\phi \sim 0$, so that $\omega = V/c$. This is the result expected since in this case the unwinding velocity V equals the circular velocity of the lift-off point, which is given by $c\omega$. Obviously the winding angle is, strictly speaking, different from zero even on parallel packages, since a winding angle of exactly zero would imply that the yarn forms a disk. The actual angle ϕ can be estimated simply for closed parallel winding, where the winding angle is such that the yarn in each layer forms a dense helix. In a package of radius $c = 200$ mm and yarn diameter $d = 0.2$ mm, one obtains $\phi \sim 0.2/2\pi \cdot 200 \sim 0.01^\circ$. Angle ϕ is therefore so small that it can be considered equal to zero for all practical purposes. Packages with a somewhat larger winding angle ϕ can also be considered as parallel. Real cross-wound packages are those with a winding angle so large that one may observe characteristic oscillations of the angular velocity during the unwinding and associated oscillations of the yarn tension (**Figures 16 and 17**). The findings can be taken into account when comparing package designs. In parallel packages one has $\phi \sim 0$, whereas in cross-wound packages parameter $\phi \neq 0$. During unwinding in the forward direction (toward the eyelet), one has $\phi < 0$, while during unwinding in the backward direction (toward the rear end of the package), one has $\phi > 0$ (**Figure 1**). Parameters V and c are known, hence we can compute the relation between the tension and angular velocity. We performed a series of experimental measurements for different unwinding velocities V and package radii c to determine the relation between the tension and angular velocity. We thus obtained the tension for a range of angular

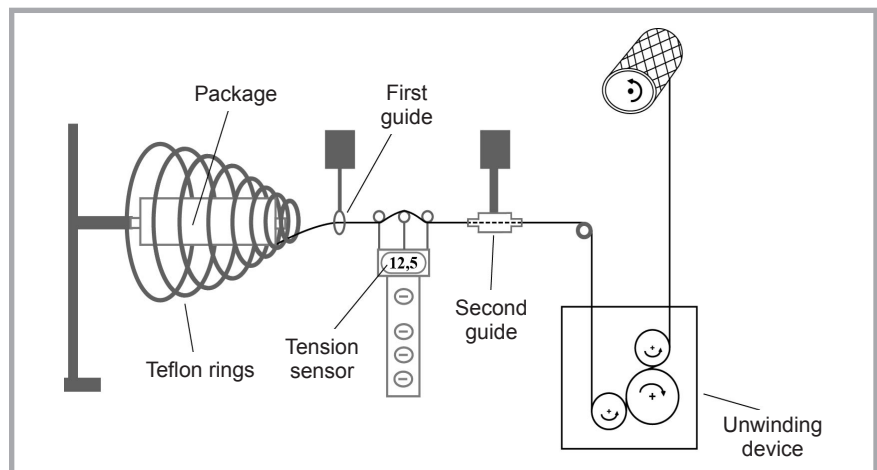


Figure 2. System for unwinding yarn from a fixed package.

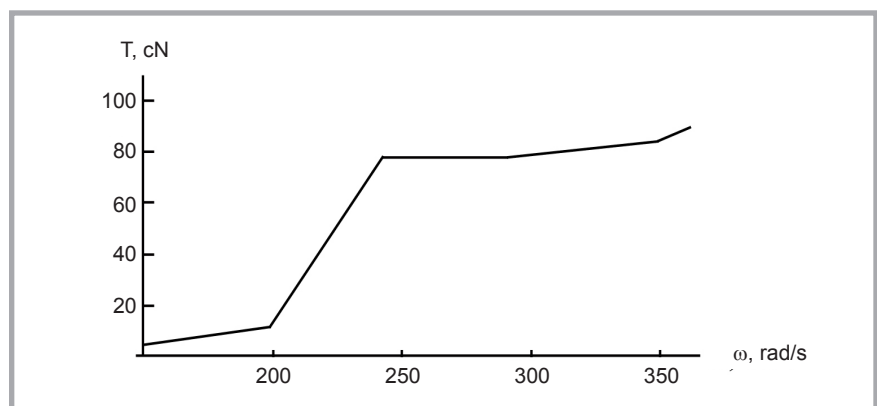


Figure 3. Dependence of tension T on the angular velocity ω of the yarn.

velocities and we used a linear interpolation between these values to obtain the relation for the whole interval of values of interest (**Figure 2**). If during the simulation, the value of ω is outside this interval, we can use a linear extrapolation for values above the highest ω measured and a quadratic extrapolation for those below the lowest ω measured.

In building this model we make a few assumptions:

1. The length of the yarn in the balloon has no effect on the tension.
2. We neglect the residual tension of yarn in the package, which is related to the stiffness of the winding.
3. The winding angle and number of threads are approximately constant in the number of layers whose unwinding will be simulated.

The dependence of T on ω was based on experimental results for a cylindrical parallel wound package with cotton yarn 41.6 tex. At low ω , up to approximately $\omega = 240$ rad/s, the tension increases approximately quadratically. After the lim-

iting value of $\omega = 240$ rad/s, the tension is bounded and increases only slightly, which is a direct consequence of using the balloon limiter in the measurements: at the limiting value of the angular velocity the radius of the balloon becomes large enough that it is limited by the balloon’s limiter. The centrifugal forces then no longer increase with ω and the tension can only grow due to yarn friction with the surface of the limiter and other less controllable reasons. Since similar balloon limiters are also used in the actual industrial process, it is advantageous to take them into account in our model.

Results of unwinding simulation

We now present the effects of different unwinding velocities V , winding angles ϕ and package radii c on tension oscillations in yarn unwinding from packages.

Cylindrical packages

In **Figure 4** we compare the tension T_0 during the unwinding of yarn from cylindrical packages at the unwinding veloc-

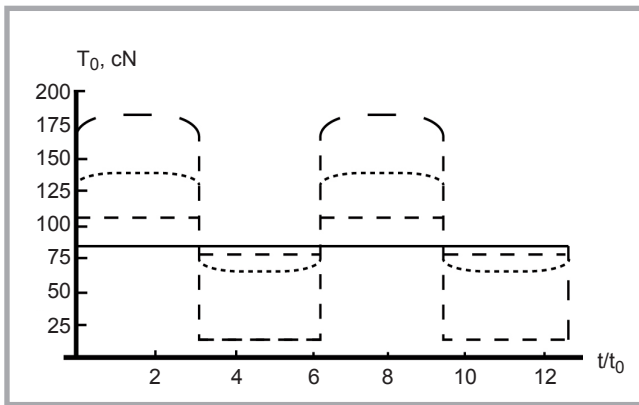


Figure 4. Variation in tension T_0 at $V = 1400$ m/min, $c = 70$ mm. $\phi \sim 0^\circ$ (full line), $\phi = 10^\circ$ (dashed line), $\phi = 20^\circ$ (dotted line), $\phi = 30^\circ$ (dot-dashed line)

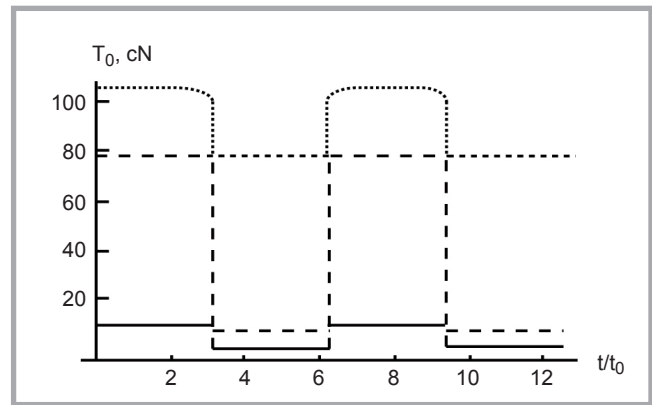


Figure 5. Variation in tension T_0 at $V = 2000$ m/min, $\phi = 10^\circ$. $c = 200$ mm (full line), $c = 150$ mm (dashed line), $c = 100$ mm (dotted line).

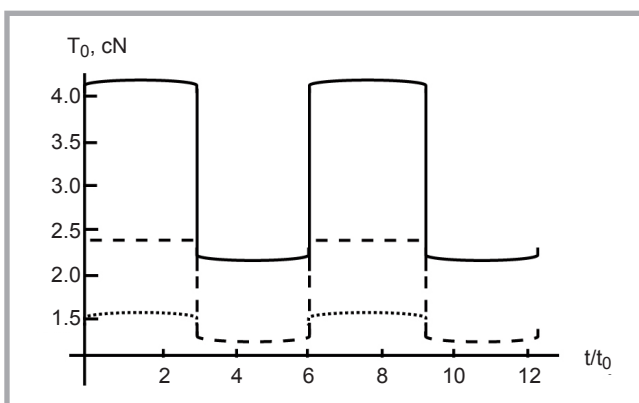


Figure 6. Variation in tension T_0 at $V = 2000$ m/min, $\phi = 10^\circ$. $c = 300$ mm (full line), $c = 400$ mm (dashed line), $c = 500$ mm (dotted line).

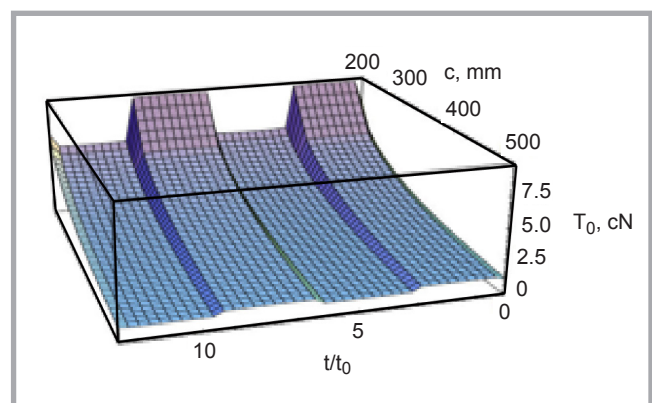


Figure 7. Tension during unwinding from a package at $V = 2000$ m/min, $\phi = 5^\circ$, $c = 200 - 500$ mm.

ity $V = 1400$ m/min and package radius $c = 70$ mm for different winding angles: $\phi \sim 0^\circ$, $\phi = 10^\circ$, $\phi = 20^\circ$ and $\phi = 30^\circ$. In parallel-wound cylindrical packages the tension is simply constant, which is expected since the winding angle in parallel-wound packages is constant at all times. In cross-wound cylindrical packages the tension in the yarn oscillates, which is due to the fact that during unwinding in the backward direction the angular velocity is higher than during that in the forward direction, which is in agreement with *Equation 2* [14]. As the yarn tension strongly depends on the angular velocity, the result is tension oscillation.

We observe that the oscillations are large. At the winding angle $= 30^\circ$, the tension varies from $T_0 = 11$ cN to $T_0 = 180$ cN. At the moment when the unwinding direction changes, the tension undergoes an almost discontinuous change. Such abrupt changes strain the yarn, therefore it is conceivable that the yarn undergoes some damage in the process. In the worst

case, the yarn can even break. At this velocity, unwinding from a package with a radius of $c = 70$ mm would not be possible.

The unit of time is chosen so that the time 2π corresponds to one period of the yarn unwinding from the package. The time on the horizontal axis is expressed in units of t_0 . The quantity t_0 is equal to the duration of one period, i.e., one cycle of the movement of the lift-off point from the front to the back edge and back, divided by 2π . Thus the time t/t_0 is the phase of motion of the lift-off point on the package surface. Namely the time 2π corresponds to precisely one cycle.

If we opt, instead, for packages with a large radius, the characteristics become quite acceptable. In *Figure 5* we compare the oscillations of tension for a high unwinding velocity $V = 2000$ m/min from cross-wound packages of winding angle $\phi = 10^\circ$ for different values of the package radius: $c = 200$ mm, $c = 150$ mm and $c = 100$ mm. At $c = 200$ mm, the ten-

sion never exceeds 20 cN. In *Figure 5* we plot the results for unwinding from packages with very large radii: $c = 300$ mm, $c = 400$ mm and $c = 500$ mm. We notice that for such packages the tension remains very small, from 1.5 cN to 4 cN.

In *Figure 7* we show the variation in tension during the unwinding of yarn at $V=2000$ m/min from a cross-wound package of winding angle $\phi = 5^\circ$, maximal package radius $c = 500$ mm and tube radius $c = 200$ mm. The figure makes it clear that it is possible to unwind the yarn even at high velocity while still maintaining a low yarn tension of 8 cN.

In *Figures 8* and *9* we show the results for the same unwinding velocity and winding angle as in *Figure 7* but for a cross-wound package of outer radius $c = 500$ mm and tube radius $c = 70$ mm. For such a package design the tension is much higher than in the previous case. When the radius decreases below 180 mm the tension noticeably increases, and at a radius below 160 mm it reaches

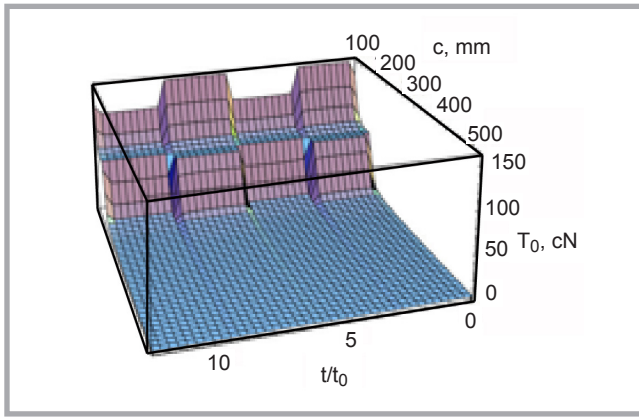


Figure 8. Tension during unwinding from a package of radius $c = 500$ mm at $V = 2000$ m/min, $\varphi = 5^\circ$, $c = 70 - 500$ mm.

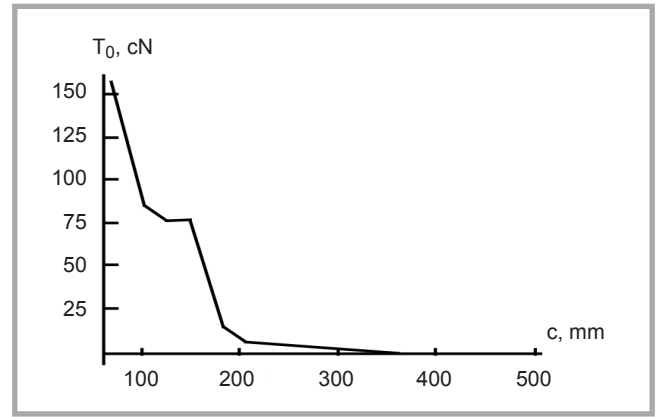


Figure 9. Tension during unwinding at $V = 2000$ m/min. Cross-section of the plot in **Figure 4.10** at $t = \pi/2$, when tension in the yarn is the largest. $\varphi = 5^\circ$.

75 cN. As the unwinding proceeds the tension rises up to 150 cN, at which the yarn would almost certainly break.

Hence we conclude that *the yarn tension can be strongly reduced by making use of packages with a large radius*, which can be demonstrated in yet another way. Let us consider a package where the tube radius is 70 mm, while that of the outermost yarn layer is 200 mm. In **Figure 10** we show unwinding from such a package, where we can observe the increasing angular velocity. As a consequence, very high tension in the yarn occurs rapidly. When the unwinding is half completed the tension has already risen up to 80 cN,

while toward the end of the unwinding amounts to 140 cN. Such high tension induces yarn damage or even breakage. Based on the results presented in **Figure 9** we may estimate that the minimal package radius should be around 150 mm in order to keep the yarn tension below 50 cN.

The choice of a limit tension of 50 cN is based on the requirement for deformations in the yarn to be in the elastic regime described by Hooke's law. The requirement implies that the tension should be such that it does not exceed 10% of the breaking strength. The choice for these values is based on the results of the ex-

perimental work. During the unwinding test, we applied up to 17% of the breaking strength to the yarn, and using the tension test we determined that the breaking force limit and elongation at break of the unwound yarn had not changed appreciably. The breaking strength of the yarn was found to be 4.5 N = 450 cN, thus the limiting value for tension during the unwinding can be estimated to be around 50 cN.

Figure 11 shows the unwinding process for a very large package with an initial radius of $c = 500$ mm and innermost layer radius of $c = 150$ mm. Again in this case the tension rapidly increases. Neverthe-

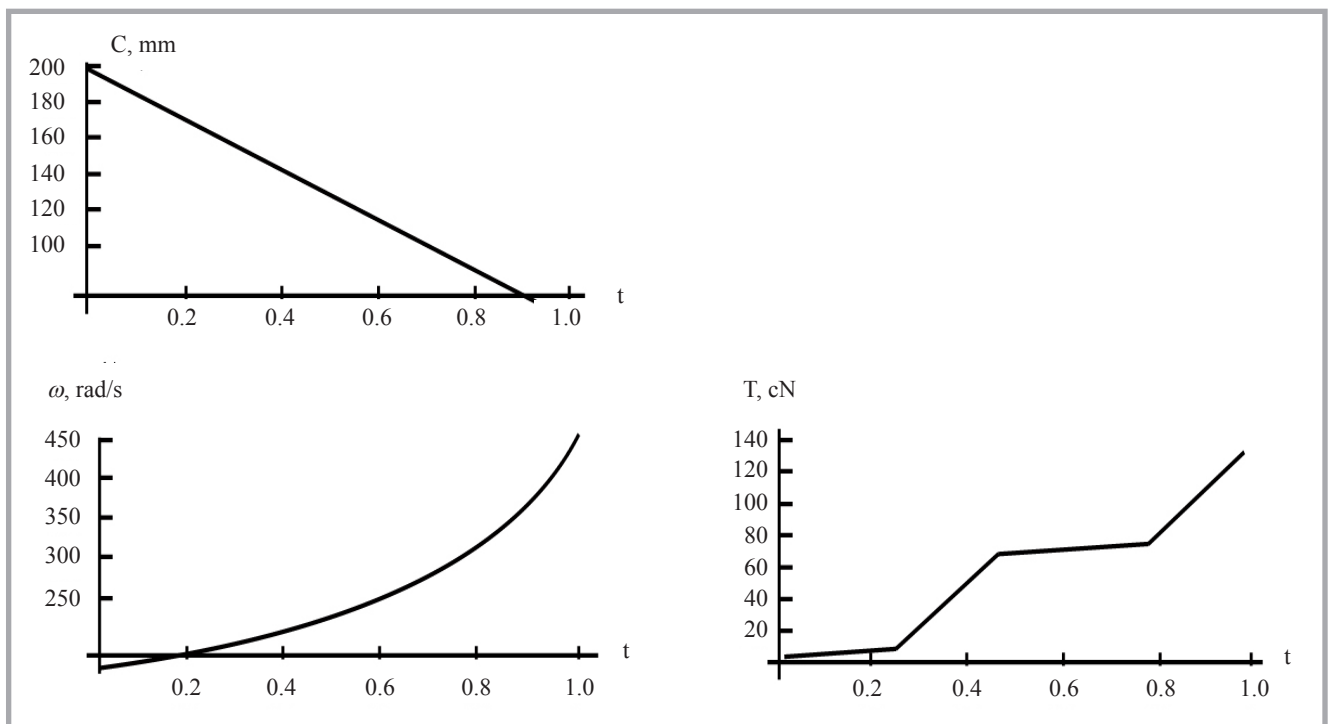


Figure 10. Variation in the radius of the top-most layer, in the angular velocity and in the tension in the yarn during unwinding from a parallel-wound cylindrical package at $V = 2000$ m/min. The tube radius is 70 mm and the outer layer radius - 200 mm.

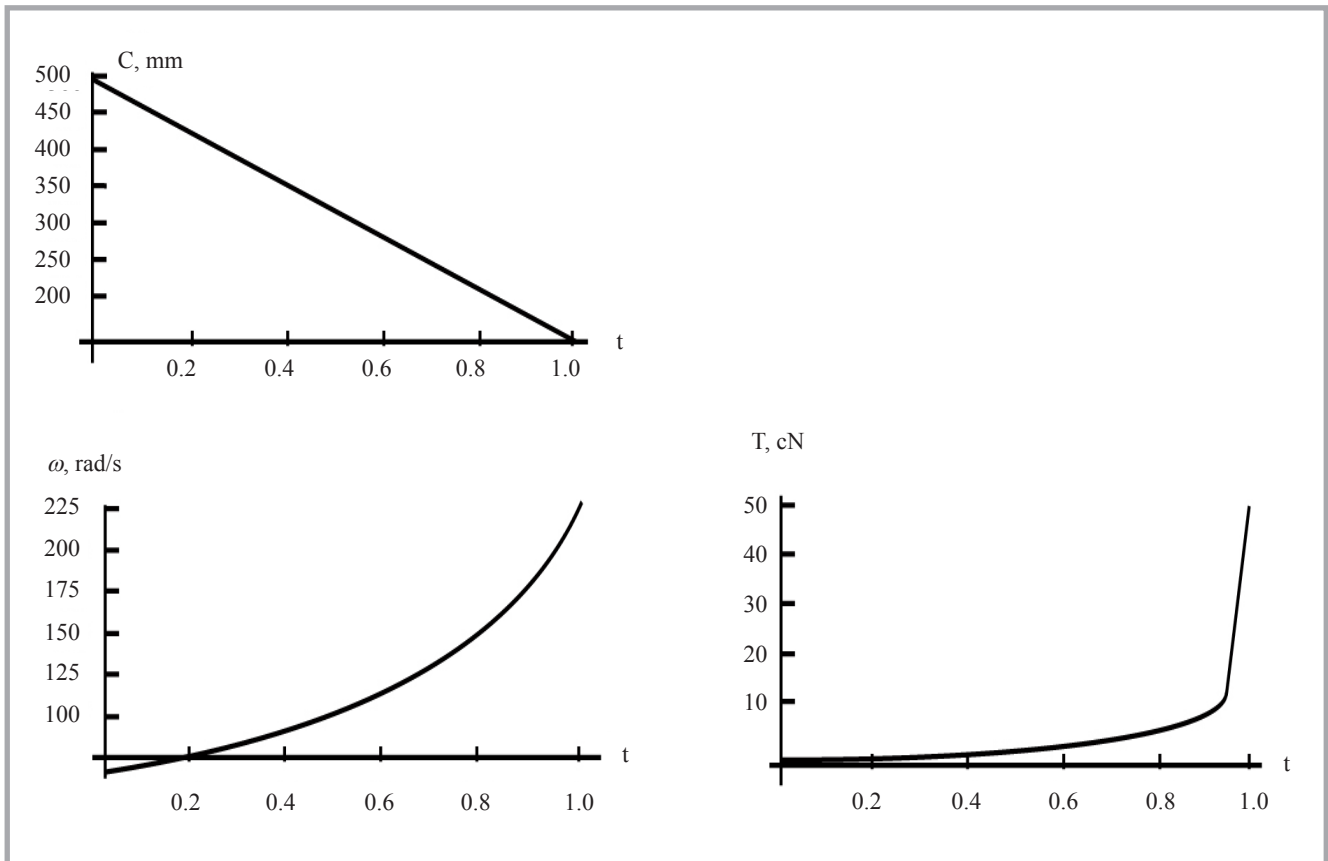


Figure 11. Variation in the radius of the top-most layer, in the angular velocity and in the tension in the yarn during unwinding from a parallel-wound cylindrical package at $V = 2000$ m/min. The outer radius is now 500 mm, while the tube radius is 160 mm.

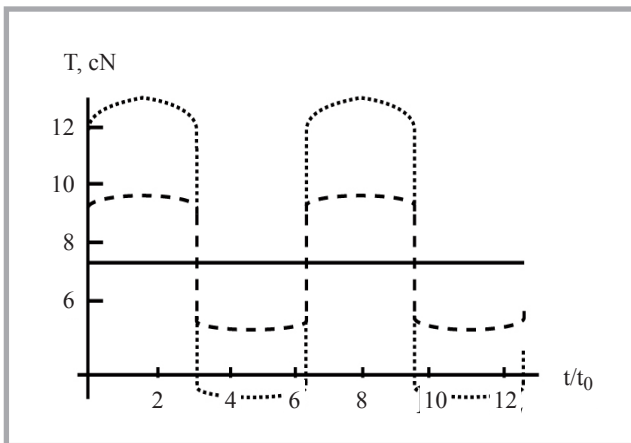


Figure 12. Tension at $V = 2000$ m/min for a range of winding angles at $c = 200$ mm. $\phi \sim 0^\circ$ (full line), $\phi = 5^\circ$ (dashed line), $\phi = 10^\circ$ (dotted line).

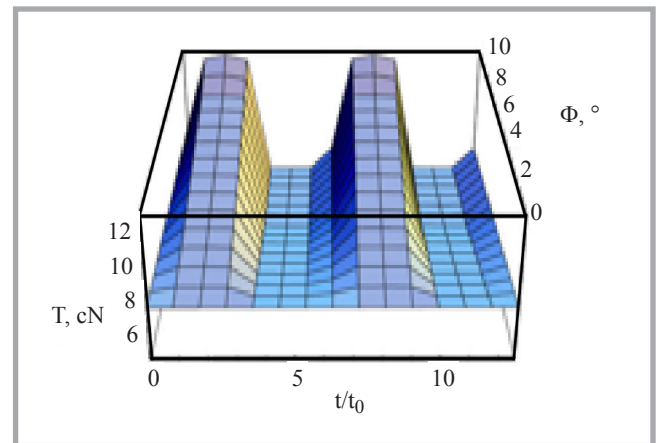


Figure 13. Tension at $V = 2000$ m/min for a winding angle range from $\phi \sim 0^\circ$ to $\phi \sim 10^\circ$ and $c = 200$ mm.

less at all times we find $\omega < 200$ rad/s. From **Figure 10** we may deduce that for such angular velocities the tension remains relatively small. Towards the end of the unwinding, a regime of $\omega > 200$ rad/s is reached and the tension rises to its maximal value of $T_0 = 50$ cN, which is precisely the acceptable maximal tension.

For a package radius of $c = 200$ mm, in **Figure 12** we compare the time variation

of the tension for three winding angles $\phi \sim 0^\circ$, $\phi = 5^\circ$ and $\phi = 10^\circ$. The unwinding velocity is 2000 m/min. For all winding angles the yarn tension is acceptable, which is also clearly demonstrated in **Figure 13**, where the parameters are the same as in **Figure 12**, but the winding angle is changed continuously from 0° to 10° .

In **Figure 14** we compare the time dependence of the yarn tension for three

package radii $c = 500$ mm, $c = 300$ mm and $c = 160$ mm, and for three winding angles 0° , 5° and 10° at an unwinding velocity of $V = 2000$ m/min. For package radii 500 mm and 300 mm we find suitable tensions $T_0 = 1.5$ cN and $T_0 = 3 - 4$ cN for all winding angles. For a package radius of 160 mm we find acceptable tension only for winding angles $\phi \sim 0^\circ$ and $\phi = 5^\circ$: in these cases the tension rises to 55 cN at most, which is at the higher end of the acceptable values. At

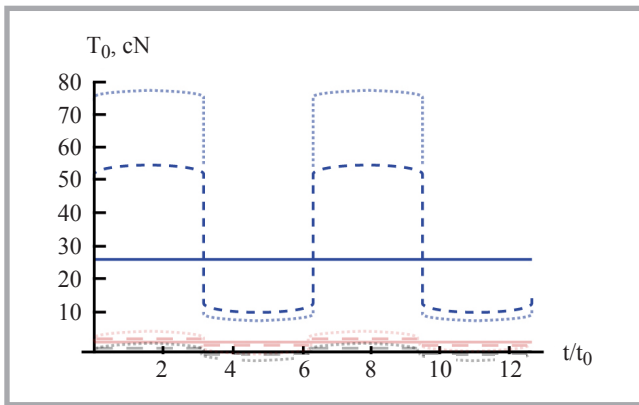


Figure 14. Tension at $V = 2000$ m/min for a range of winding angles and package radii. Package radii are $c = 500$ mm (black), $c = 300$ mm (red), $c = 160$ mm (blue). Winding angles: $\phi \sim 0^\circ$ (full line), $\phi = 5^\circ$ (dashed line), $\phi = 10^\circ$ (dotted line).

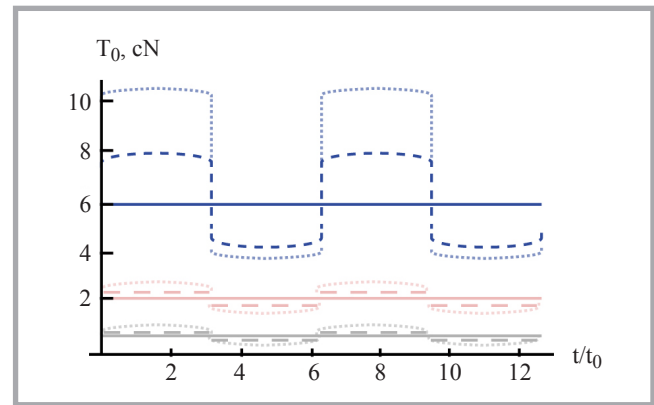


Figure 15. Tension at $V = 1500$ m/min for a range of winding angles and package radii. Package radii are $c = 500$ mm (black), $c = 300$ mm (red), $c = 160$ mm (blue). Winding angles: $\phi \sim 0^\circ$ (full line), $\phi = 5^\circ$ (dashed line), $\phi = 10^\circ$ (dotted line).

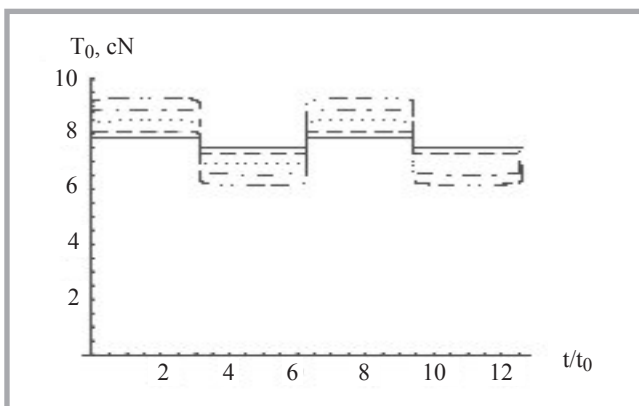


Figure 16. Tension T_0 for different winding angles. $V = 2000$ m/min and $c = 200$ mm. $\phi \sim 0.5^\circ$ (full line), $\phi = 1^\circ$ (dashed line), $\phi = 2^\circ$ (dotted line), $\phi = 3^\circ$ (dot-dashed line), $\phi = 4^\circ$ (dot-dot-dash-dash line).

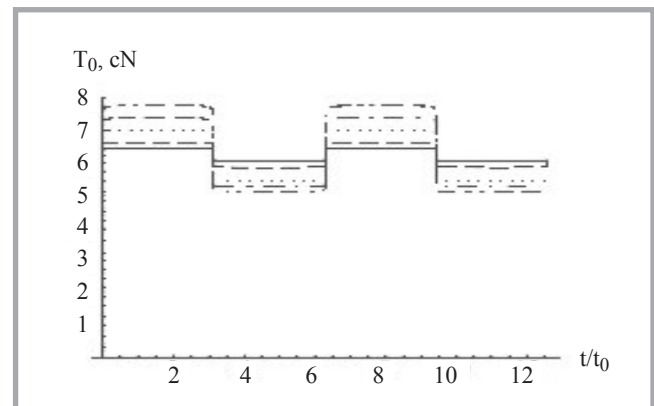


Figure 17. Tension T_0 for different winding angles. $V = 1000$ m/min and $c = 200$ mm. $\phi \sim 0.5^\circ$ (full line), $\phi = 1^\circ$ (dashed line), $\phi = 2^\circ$ (dotted line), $\phi = 3^\circ$ (dot-dashed line), $\phi = 4^\circ$ (dot-dot-dash-dash line).

$\phi = 10^\circ$ we observe tensions of around 80 cN, which exceed the limit. In **Figure 15** we also compare the time dependence of the yarn tension for the same three package radii and the same three winding angles, but for a lower unwinding velocity of $V = 1500$ m/min. For all package radii and winding angles we observe that the tension remains low.

Figures 16 and **17** present the time dependence of the tension for five winding angles: 0.5° , 1° , 2° , 3° and 4° for package radius $c = 200$ mm and for two unwinding velocities: $V = 2000$ m/min and $V = 1000$ m/min, respectively. Both figures demonstrate the transition from a regime of small winding angles of 0.5° & 1° , which are characteristic for parallel-wound packages, and where the tension oscillations tend to be negligible, to one of larger angles: 2° , 3° & 4° , where one readily observes higher tension oscillations that characterise cross-wound packages. For both unwinding velocities we

obtain small tension for all five winding angles, that is from 5 cN to 8 cN.

Conic packages

In **Figures 18** and **19** we show the variation in tension during unwinding from conic packages for three different apex angles: $\alpha = 0^\circ$, $\alpha = 5^\circ$ and $\alpha = 10^\circ$ and for two different radii: $c = 200$ mm and $c = 500$ mm. The winding angle is $\phi = 10^\circ$ and the unwinding velocity - $V = 200$ m/min.

The conclusion is that the influence of the apex angle on the tension variation is negligible.

Simulation of unwinding from new generation packages with interleaved layers of parallel and cross winding

It is also possible to construct packages with a mixed layer structure, for instance packages where there is an alternation of layers with cross and parallel winding. The package should be designed such

that the parallel layers are unwound in the backward direction, while the intermediate cross wound layers should be unwound in the forward direction. This choice is based on the observation that cross winding leads to high tension during unwinding in the backward direction. The additional benefit of cross-wound layers between two parallel layers is that the yarn in the cross-wound sections prevents the parallel layers from interleaving.

In **Figure 20** we show the changing yarn tension during unwinding from regular cross-wound packages and from new-generation packages. The parameters are the unwinding velocity $V = 2000$ m/min and $c = 200$ mm. The angle of cross-wound layers in both packages is $\Phi = 10^\circ$. We observe that the parallel layers in the new packages strongly reduce the tension oscillations, as we had expected. Instead of tensions in the range from 5 cN to 13 cN, in the new packages we find tensions between 5 cN to 8 cN. We

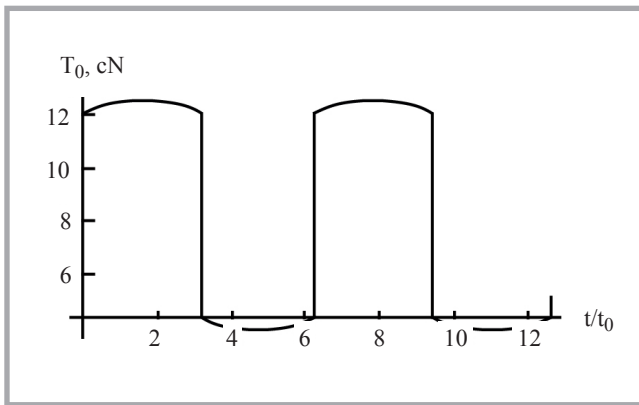


Figure 18. Tension for conic packages of radius $c = 200$ mm and winding angle $\varphi = 10$ at unwinding velocity $V = 2000$ m/min for different apex angles. $\alpha = 0^\circ$ solid line, $\alpha = 5^\circ$ dashed line, $\alpha = 10^\circ$ dotted line.

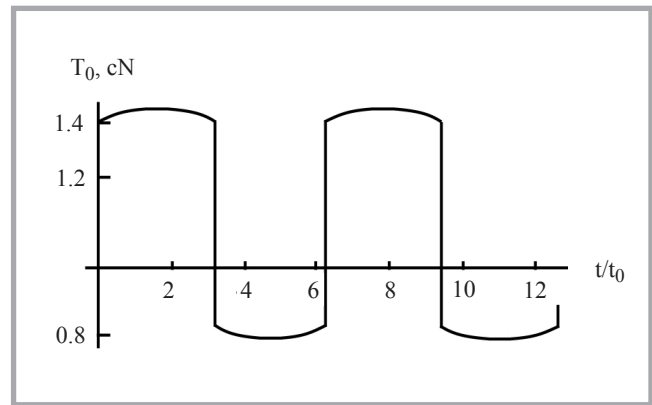


Figure 19. Tension for conic packages of radius $c = 500$ mm and winding angle $\varphi = 10$ at unwinding velocity $V = 2000$ m/min for different apex angles. $\alpha = 0^\circ$ solid line, $\alpha = 5^\circ$ dashed line, $\alpha = 10^\circ$ dotted line.

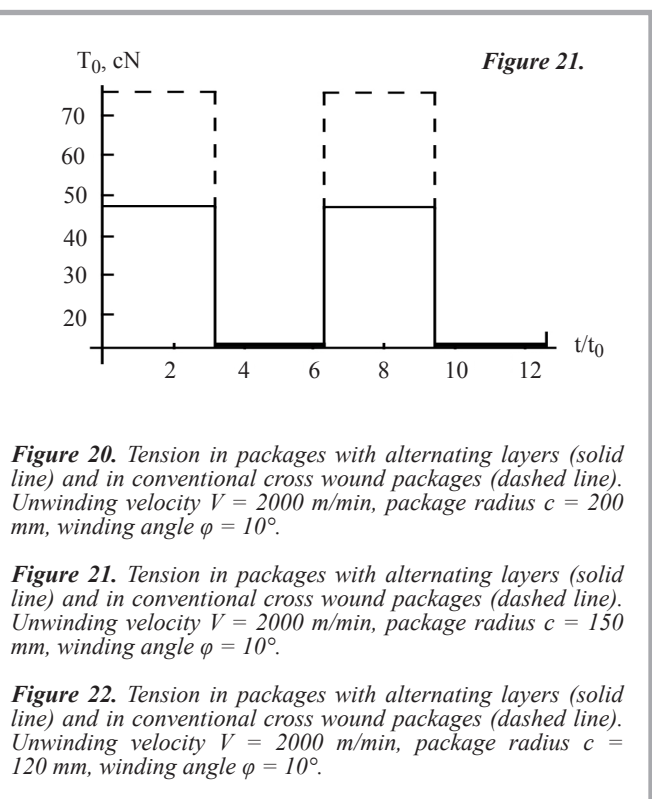
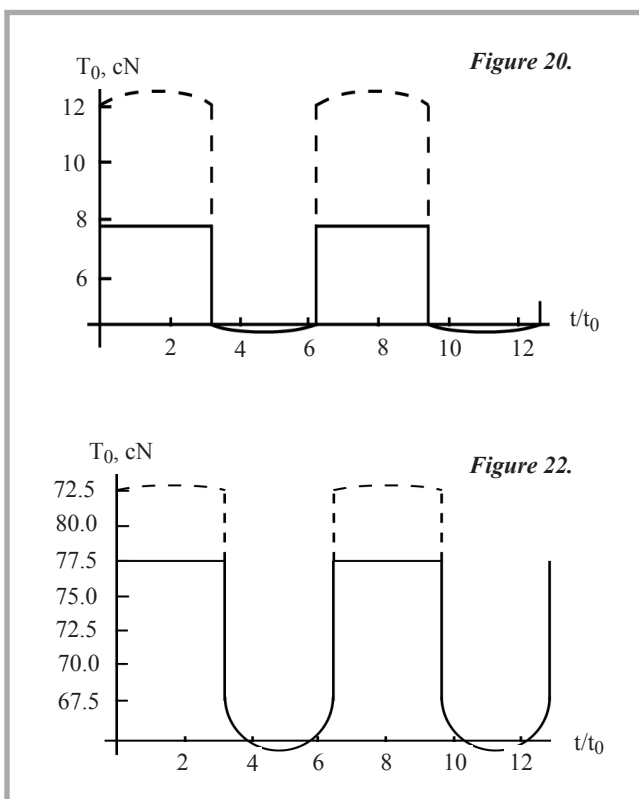


Figure 20. Tension in packages with alternating layers (solid line) and in conventional cross wound packages (dashed line). Unwinding velocity $V = 2000$ m/min, package radius $c = 200$ mm, winding angle $\varphi = 10^\circ$.

Figure 21. Tension in packages with alternating layers (solid line) and in conventional cross wound packages (dashed line). Unwinding velocity $V = 2000$ m/min, package radius $c = 150$ mm, winding angle $\varphi = 10^\circ$.

Figure 22. Tension in packages with alternating layers (solid line) and in conventional cross wound packages (dashed line). Unwinding velocity $V = 2000$ m/min, package radius $c = 120$ mm, winding angle $\varphi = 10^\circ$.

have thus achieved an elimination of high tension spikes which lead to yarn breaking in conventional cross-wound packages. For this reason, new-generation packages would allow unwinding at higher velocities, as compared to traditional packages.

We also notice that the mixed structure of the new packages allows to chose a larger winding angle, even up to 10° . Cross-winding is used in layers which are unwound in the forward direction, where we generally find lower yarn tensions. Parallel-winding is used, however, in layers which are unwound in the back-

ward direction. If these layers were cross-wound, as in conventional packages, the tension would spike during unwinding.

The variation in tension in conventional cross-wound packages and in new-generation packages is shown in **Figure 21**. The unwinding velocity is the same as in the previous figure, but now the package radius is smaller - $c=150$ mm. In the new packages the maximal tension is below 50 cN. We thus conclude that in this type of package, unwinding is also possible at this package radius.

Assuming that the yarn can sustain tensions of up to 15% of the breaking ten-

sion, as suggested by experimental results, we can set a new upper limit for acceptable values of the yarn tension, that is, 75 cN. With this value and using the new package design, it is possible to reduce the package radius even further. As an example, in **Figure 22**, we show unwinding from a package of radius $c = 120$ mm at an unwinding velocity of $V = 2000$ m/min. In new-generation packages the maximal tension found is 78 cN, which is probably still acceptable, while in classical packages it would be somewhat higher - 82 cN. The conclusive answer to the question if these unwind-

ing parameters are suitable, would only be determined experimentally.

We may conclude that the new-generation packages allow unwinding at very high velocities without excessive tension oscillations, which are the main disadvantage of conventional cross-wound packages.

■ Conclusion

We have shown that a combination of theoretical modelling and an empirically determined relation between the yarn tension and angular velocity of yarn in the balloon can be used to determine a suitable set of parameters for unwinding from packages of various designs. We have reached the following conclusions:

- In cross-wound packages, when the yarn unwinds backwards the angular velocity is higher than when the yarn unwinds forwards, which leads to oscillations in the yarn tension. Abrupt changes in tension occur at the edges of the package.
- Unwinding at high velocity (2000 m/min) from regular cross-wound packages is impossible for package radii below 150 mm.
- Oscillations of tension are smaller in packages with a small winding angle (parallel-wound packages), but for such packages yarn slips can occur during unwinding.
- Alternatively the oscillations of tension can be reduced only if those layers of yarn that are unwound backwards are wound in parallel.

Using packages with alternating layers of parallel and cross wound yarn, both the maximum tension and tension oscillations can be significantly reduced. In this case it is possible to safely unwind from packages of smaller radius even at higher unwinding velocities, which would allow higher production rates without increased down-time due to yarn breaking.

We have determined that it is possible to safely unwind yarn from packages with alternating layers of 150 mm radius and in some circumstances even 120 or 100 mm.



References

1. Padfield DG. A note on fluctuations of tension during unwinding. *J. Text. Inst.* 1956; 47: 301-308.

2. Padfield DG. The Motion and Tension of an Unwinding Thread. *Proc. R. Soc.* 1958; A245: 382-407.
3. Kothari VK, Leaf GAV. The unwinding of yarns from packages, Part I: The theory of yarn-unwinding. *J. Text. Inst.* 1979; 70(3): 89-95.
4. Kothari VK, Leaf GAV. The unwinding of yarns from packages, Part II: Unwinding from cylindrical packages. *J. Text. Inst.* 1979; 70(3): 96-104.
5. Fraser WB, Ghosh TK, Batra SK. On unwinding yarn from cylindrical package. *Proc. R. Soc. Lond. A.* 1992; 436: 479-498.
6. Fraser WB. The effect of yarn elasticity on an unwinding balloon. *J. Text. Inst.* 1992; 83: 603-613.
7. Clark JD, Fraser WB, Stump DM. Modelling of tension in yarn package unwinding. *J. Engi. Mathema.* 2001; 40: 59-75.
8. Ghosh TK, Batra SK, Murthy AS. Dynamic Analysis of Yarn Unwinding from Cylindrical Packages, Part I: Parametric Studies of the Two-Region problem. *Textile Research Journal* 2001; 71: 771-778.
9. Ghosh TK, Batra SK, Murthy AS. Dynamic Analysis of Yarn Unwinding from Cylindrical Packages, Part II: The Three-region Analysis. *Textile Research Journal* 2001; 71, 10: 855-861.
10. Kim K-W, Lee J-W, Yoo W-S. Effect of gravity and tangential air resistance on unwinding cable. *Nonlinear Dynamic* 2012; 70, 1: 67-87.
11. Shim WS, Lee H, Lee DW. *The Interaction of Moving Yarns with Stationary Surfaces. Fibres and polymers* 2013; 14, 1, 164-171.
12. Kim K-W, Lee JW, Yoo W-S. Unwinding characteristics of thin cables for inner and outer dispensers. *Nonlinear Dynamic* 2013; 72, 1-2: 333-351.
13. Pracek S, Mozina K, Sluga F. Shock in the yarn during unwinding from packages. *Abstract and Applied Analysis* 2013; art. ID 972941, 6 pages. <http://dx.doi.org/10.1155/2013/972941>, doi: 10.1155/2013/972941.
14. Kong XM, Rahn CD, Goswami BC. Steady-state unwinding of yarn from cylindrical packages. *Text. Res. J.* 1999; 69, 4: 292-306.
15. Pracek S. Theory of string motion in the textile process of yarn unwinding. *International Journal of Nonlinear Sciences and Numerical Simulation* 2011; 8, 3: 451-460, DOI: 10.1515/IJNSNS.2007.8.3.451.

■ Received 22.07.2013 Reviewed 31.07.2014



Textile Research Institute (IW) in Lodz is the oldest research & development centre of textile industry in Poland. In the year 2015 we celebrate the 70-th anniversary of its establishment.

The 70 years of successful work and continuous development would not be possible without cooperation with industrial partners, many Polish and international research centres and universities, without the participation in international research programmes, in the framework of scientific networks, and without the support of many institutions and individuals during all these years.

We hope that the celebration of the jubilee of Textile Research Institute, which will be held in Łódź on June 16-th this year, will be a special opportunity to express our gratitude and warmly thanks for all who participated in the development of the Institute and who are nowadays creating the new face of textile industry.